Available online at www.sciencedirect.com
ScienceDirect
Trans. Nonferrous Met. Soc. China 25(2015) 3354−3362
Transactions of Nonferrous Metals Society of China
www.tnmsc.cn

Sliding wear behavior of copper-based composites reinforced with graphene nanosheets and graphite

Jing-fu LI, Lei ZHANG, Jin-kun XIAO, Ke-chao ZHOU

State Key Laboratory of Powder Metallurgy, Central South University, Changsha 410083, China

Received 27 November 2014; accepted 29 April 2015

Abstract: The mechanical and tribological properties of hot-pressed copper-based composites containing different amounts of graphene nanosheets (GNSs) are compared with those of copper−graphite (Gr) composites fabricated by the same method. The results show that the Cu−GNSs composites exhibit higher relative density, microhardness and bending strength compared with Cu−Gr composites with the same volume fraction of GNSs and Gr. Moreover, the friction coefficients and wear rates reduce significantly by the addition of GNSs, whereas the limited impact on reducing friction and wear is found on graphite. The abrasive and delamination wear are the dominant wear mechanisms of the composites. It is believed that the superior mechanical and tribological performances of Cu−GNSs composites are attributed to the unique strengthening effect as well as the higher lubricating efficiency of graphene nanosheets compared with those of graphite, which demonstrates that GNS is an ideal filler for copper matrix composites, acting as not only an impactful lubricant but also a favorable reinforcement.

Key words: graphene nanosheets; graphite; composite; friction coefficient; wear mechanism

1 Introduction

The inherent properties of copper, such as high thermal and electric conductivity, along with the self-lubricating property of graphite made copper−graphite composites to be a high-performance material, which has been widely used in many industrial applications, such as brushes, contact strips and bearing materials [1−3]. However, it is well known that the lubricating property of graphite is extrinsic [4], what's more, in order to obtain low friction and wear, numerous amount of graphite is needed to be incorporated into copper, which lowers the mechanical properties (i.e., hardness and fracture strength) of the composites [5−7]. In present time, with increasing the complexity, the power usage and serve life of the aforementioned applications, minimizing friction and wear-related mechanical failures in such moving mechanical assemblies remains to be an issue of global concern [8]. An intense effort is underway to find novel materials and lubricants that can potentially avoid friction's adverse impacts on efficiency and reliability [9,10] and the discovery of graphene may give the way to control friction and wear due to its impressive thermal, electrical, mechanical and tribological properties [11−14].

In recent years, more and more dedicated investigations have been realized and or have demonstrated the remarkable tribological performance of graphene. SHIN et al [15] have determined the ultralow friction coefficient (approximately 0.03) of exfoliated and epitaxial graphene in micro-scale scratch tests under ambient conditions. Moreover, unlike other solid lubricants such as MoS_2, WS_2 or graphite, a small amount of graphene is sufficient to reduce both friction and wear due to its high lubricating efficiency [16]. Solution-processed graphene, which is deposited from ethanol solution with low concentration (1 mg/L), has been detected to have anti-corrosion property in the case of steel against steel both in dry nitrogen and humid air environments due to the formation of a conformal protective coating on the sliding interface, which facilitates shear and slows down the tribo-corrosion [17,18]. More importantly, researches on graphene reinforced ceramic [19], glass [20] and polymer composites [21] are gaining high momentum. PORWAL et al [16] have investigated the tribological properties and wear mechanisms of silica−graphene nano platelet (GNP) composites, and the results clearly demonstrated that a percolating network of GNP above a critical concentration provided a lubricating effect to the silica matrix resulting in the decline of the friction coefficient

Corresponding author: Lei ZHANG; Tel: +86-731-88830464; E-mail: zhanglei@csu.edu.cn
DOI: 10.1016/S1003-6326(15)63970-X

by ~20% while increasing the wear resistance of the composite by ~5.5 times compared with pure silica, and micro-fracture along with wear debris was observed as the main wear mechanism for silica−graphene nano platelet composites. Graphene is also employed as an oil additive, providing elevated lubricating properties, which hinders friction and wear under a wide scope of test conditions [22]. All of these researches indicate the great competence and potential of graphene as a solid lubricant that can minimize friction and wear in various tribological applications.

It should be noted that the limited effort has been put forth in the study of tribological properties of metal matrix−graphene composites [14,23], and the superiority and applicability of graphene acting as a lubricant in metal matrix are not fully understood. This work emphasizes on the mechanical and tribological properties of copper-based composites with different volume fractions of graphene. In order to evaluate the anti-wear performance of graphene, the obtained results are compared with copper−graphite composites fabricated by the same method.

2 Experimental

2.1 Material preparation

The commercially supplied graphene powder was suspended in acetone and sonicated using ultrasonic dispersing technology for more than 6 h until the suspension with homogeneous distribution of graphene particles was obtained. After sonication, the commercially available electrolytic copper powder (99.98% purity with average particle size of 25 μm) was added to the aforementioned suspension and mixed using magnetic stirring technology, meanwhile the slurry was dried at 30 °C in a vacuum drying oven for 4 h. The powder morphologies of graphite (Gr), graphene nanosheets (GNSs) and typical powder mixture of Cu−7.5%GNSs (volume fraction) are shown in Fig. 1. The graphite powder with an average particle size of 5 μm has a flake like morphology (Fig. 1(a)), whereas curled, wrinkled and overlapped stacks of graphene nanosheets are observed in Fig. 1(b). The well embedding of GNSs into the copper powder, as shown in Fig. 1(c), indicates the strong interface bonding between copper and GNSs in the sintered composites. The prepared composite powders were finally sintered into disks of 50 mm in diameter and 3 mm in thickness using hot pressing method at 900 °C with applying 25 MPa pressure for more than 40 min. The schematic diagram of preparation process is shown in Fig. 2. Accordingly, the copper matrix composites with graphene contents of 2.5%, 5%, 7.5% and 10% (volume fraction) were consolidated. Cu/Gr composites were also fabricated

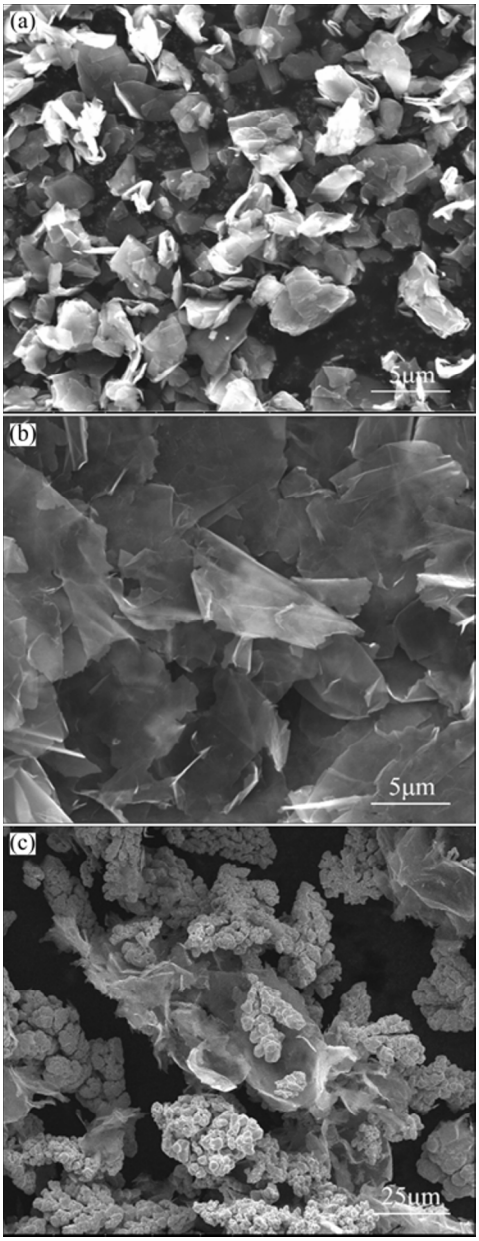

Fig. 1 SEM images of graphite (a), graphene nanosheets (b) and Cu/GNSs powder mixture (c)

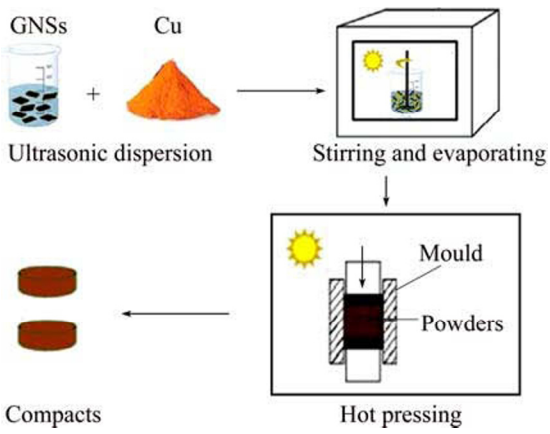

Fig. 2 Schematic diagram of preparation process of composites

through the same sintering technique for comparative study.

2.2 Mechanical and tribological performance test

The bulk densities of the composites were measured using Archimedes' method, and the corresponding relative densities were determined by means explained elsewhere [16]. The hardness of sintered composites was measured on a Vickers microhardness tester under a load of 0.25 N for 10 s. The bending strength was evaluated by a three-point bending test.

The tribological test of as-prepared flat sample was conducted under ambient condition (temperature of (20±5) °C and relative humidity of 60%±5%) using a CSM tribometer with a ball-on-disk contact geometry. The counterpart is GCr15 ball with a diameter of 6 mm. Prior to test, the samples were manually ground and finished with 800-grit silicon carbide paper and then cleaned with acetone. The applied load and sliding speed were maintained at 2 N and 1 m/s, respectively. The sliding distance was 2000 m. The coefficient of friction was continually recorded during the tests and the average value was calculated for each test within the distance of 2000 m. The wear volume was calculated from the cross section area of worn surface profile traces using a 3D digital microscope (HIROX KH−7700, Japan) according to the procedure given in the ASTM standard G99 [24] and the wear volume was then converted into the volumetric wear rate. The wear volume, V, was calculated according to the following equation:

$$V = 2\pi R\left[r^2 \sin^{-1}\left(\frac{w}{2r}\right) - \left(\frac{w}{4}\right)\sqrt{4r^2 - W^2}\right] \quad (1)$$

where V is the wear volume, R and w are the sliding radius and the average width of the wear track, and r is the radius of the counterface ball. The wear rate, W, is computed from the slope of wear volume versus sliding distance:

$$W = \frac{\Delta V}{\Delta d} \quad (2)$$

where ΔV is the wear volume within an interval of Δd sliding distance.

In order to obtain the differences between graphite and graphene nanosheets acting as a filler in the copper matrix, the fracture surfaces, worn surfaces and wear debris of the composites were analyzed by a scanning electron microscope (FEI, Nova Nano SEM 230) equipped with energy dispersive X-ray detector (EDX). Raman spectroscopy was also carried out on GNSs, as-prepared Cu−GNSs composite and worn surfaces to acquire the information of the evolution of GNSs during experiment.

3 Results and discussion

3.1 Microstructure of composites

The typical SEM images of the prepared copper−graphite and copper−graphene nanosheets composites are shown in Fig. 3. As can be seen from Fig. 3(a), the graphite particles are homogeneously distributed throughout the copper matrix. No cracks and fissures are observed in the micrograph, which confirms the good sinterability of the composites. The typical SEM images of Cu−7.5%GNSs composite (Figs. 3(b) and (c)) show the uniform distribution of GNSs in the matrix, in

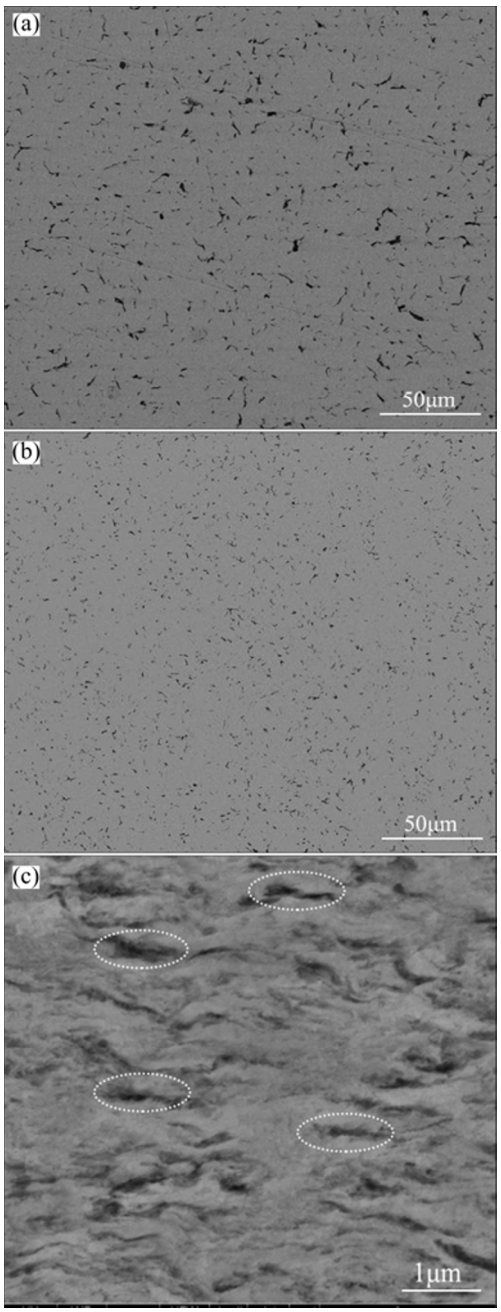

Fig. 3 Typical SEM images of composites: (a) Cu−7.5%Gr; (b) Cu−7.5%GNSs; (c) High magnification image of (b)

addition, the GNSs are securely anchored within the copper matrix to form a large area of interface. It is believed that the secure binding and better homogeneity of GNSs in the copper matrix can promote the tribological performance of the composites due to stress dissipation [25].

3.2 Mechanical properties of composites

The mechanical properties such as relative density, microhardness and bending strength of composites were investigated, as shown in Table 1. The manufacturing with hot-pressing method leads samples to be regarded as "full dense", thus the relative density is found to be 97%−99%. The Vickers microhardness of the Cu−GNSs composites increases from HV 67.8 to HV 97.4 with the addition of GNSs up to 7.5%, which is 44% enhancement over the unreinforced copper matrix. The remarkable enhancement of hardness of copper matrix achieved by introducing a small amount of GNSs could be attributed to the effect of strengthening effect of GNSs. The thermal expansion mismatch between copper and GNSs generates residual stress in the copper matrix during sintering. The residual stress results in the increase of dislocation density making the composites tougher [16,25]. However, the reduction of Vickers microhardness of the composites can be observed as the content of reinforcements reaches 10%, which indicates the degradation of strengthening effect. The bending strength of Cu−GNSs composites decreases gradually with the addition of GNSs, which can be attributed to the relatively weak interface bonding of Cu and GNSs as compared with that of copper matrix, which can be susceptible to the crack nucleation under pressure. Figure 4 shows the SEM images of fracture surfaces of the samples reinforced with different volume fractions of GNSs. As can be seen from Figs. 4(a) and (b), the GNSs in large sheets run along the grain boundaries of the copper matrix, and the pulling out of GNSs demonstrates

Table 1 Mechanical properties of Cu−Gr and Cu−GNSs composites

Volume fraction of reinforcement/%	Cu−Gr composites			Cu−GNSs composites		
	Relative density/%	Microhardness (HV)	Bending strength/MPa	Relative density/%	Microhardness (HV)	Bending strength/MPa
2.5	98.9	66.5	362.03	99.1	67.8	441.27
5	98.5	69.2	294.39	98.9	71.7	301.16
7.5	98.4	74.2	185.68	98.7	97.4	284.01
10	98.2	68.9	149.01	97.5	56.8	211.85

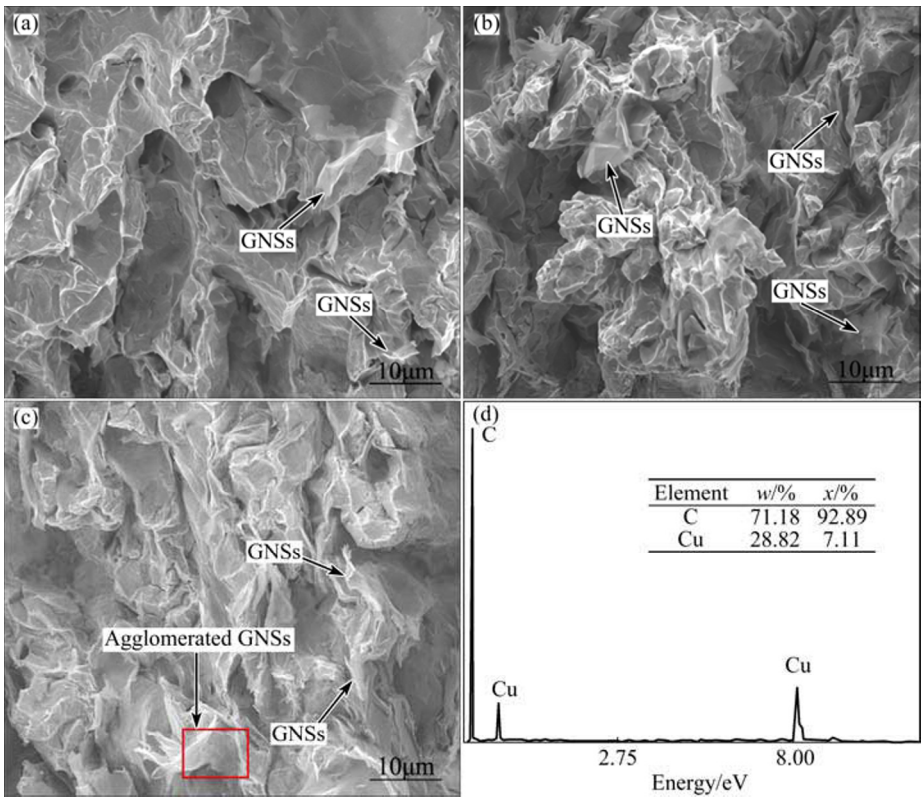

Fig. 4 SEM images of fracture surfaces of Cu−GNSs composites with 2.5% GNSs (a), 7.5% GNSs (b), 10% GNSs (c) and EDX profile (d) at interface of Cu−10%GNSs

that they are firmly bonded with the matrix. This strong interface bonding of Cu and GNSs would facilitate the stress transfer and then enhance the strength, since the applied stress is transferred to the high strength GNSs through the interface. Moreover, the high strength GNSs located along the grain boundaries can act as two dimensional obstacles to restrict the motion of dislocations in the matrix. However, the agglomeration and clustering of GNSs are observed in the Cu−10%GNSs composite, as shown in Fig. 4(c), which is because of the difficulty in evenly dispersing such amount (10%) of GNSs by stirring. Thus the non-uniformity of distribution of GNSs in the composite will weaken the effects of GNSs on the strength and toughness of the Cu matrix composite, which is responsible for the inferior mechanical properties of Cu−10%GNSs composite, such as reduced hardness and bending strength. The typical EDX profile of the interface of composites (indicated by the red square in Fig. 4(c)) shows high intensity peak of carbon and relatively low intensity peak of copper. The absence of other elements like oxygen and other interfacing reaction products confirms the good interfacial integration of Cu−GNSs composites. On the other hand, the mechanical properties of Cu−Gr composites is observed to be inferior to those of Cu−GNSs composites, besides the slight fluctuation of Vickers microhardness of Cu−Gr composites with the increment of graphite, demonstrates that the effect of graphite acting as a reinforcement in the copper matrix is in very low-grade level.

3.3 Friction and wear characteristics

Figure 5(a) shows the average friction coefficients of different composites within the sliding distance of 2000 m. It is found that the friction coefficient of Cu−Gr composites decreases from 0.28 to 0.19 with the increase of graphite in the copper matrix (Fig. 5(a)). Moreover, the frictional behavior of Cu−Gr is rather unsteady (see the coarse friction curve in the inset of Fig. 5(a)). However, the friction coefficient of Cu−GNSs composites reduces from 0.24 to 0.16 with the increase of GNSs and smaller amplitude of fluctuation of the frictional curve is observed on the Cu−GNSs composite. The enhanced stability of frictional behavior of Cu−GNSs composites demonstrates that the small amount of GNSs can provide valid lubricating effect to the Cu matrix, whereas the lubrication of such content graphite is limited. The above findings confirm the superior antifriction efficiency of GNSs compared with that of graphite.

Figure 5(b) shows the variation of wear rates of Cu−GNSs and Cu−Gr composites. For Cu−GNSs composites, the wear rate gradually decreases from 13.6×10^{-4} to 2.3×10^{-4} mm^3/m with the volume fraction

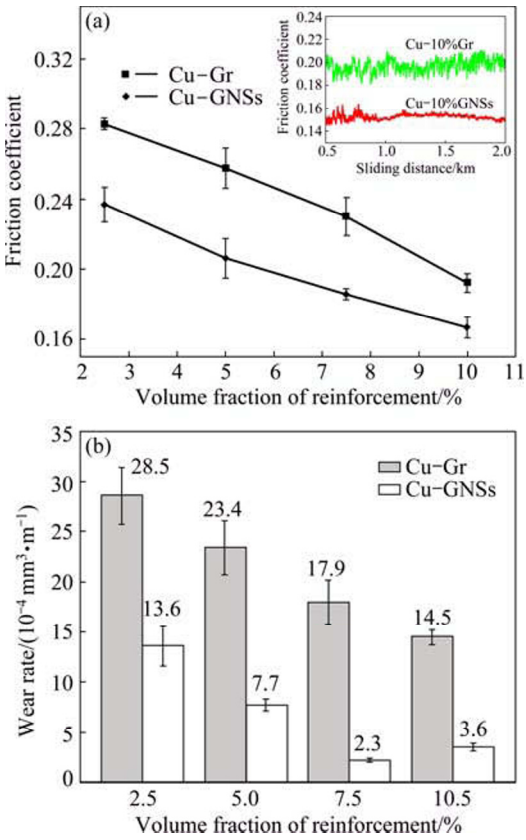

Fig. 5 Tribological properties of Cu−GNSs and Cu−Gr composites: (a) Average friction coefficients; (b) Wear rates (inset in (a) shows dynamic friction coefficients under steady state condition)

of GNSs increasing from 2.5% to 7.5%. The improvement in wear resistance can be ascribed to the strengthening and lubricating effect of GNSs to the copper matrix, which limits the removal of material during the sliding process. Nevertheless, with further increasing the volume fraction of GNSs (beyond 7.5%) in copper matrix, an increase in wear rate is observed. The degradation of anti-wear ability may be attributed to the deterioration of mechanical properties, which results in the poor load bearing ability of Cu−10%GNSs composite. As for Cu−Gr composites, the wear rates are several times higher than those of Cu−GNSs composites when the same amount of lubricant is added. This could be owing to the insignificant lubricating effect of the small amount of graphite to the copper matrix, on the other hand, no obvious reinforcement is found in the Cu−Gr composites.

3.4 Wear mechanism

For deeper understanding of the effect of GNSs on the tribological performances and the distinction between graphene nanosheets and graphite acting as a lubricant, SEM micrographs of worn surfaces of the composites are obtained, as shown in Fig. 6. Figures 6(a) and (b) show

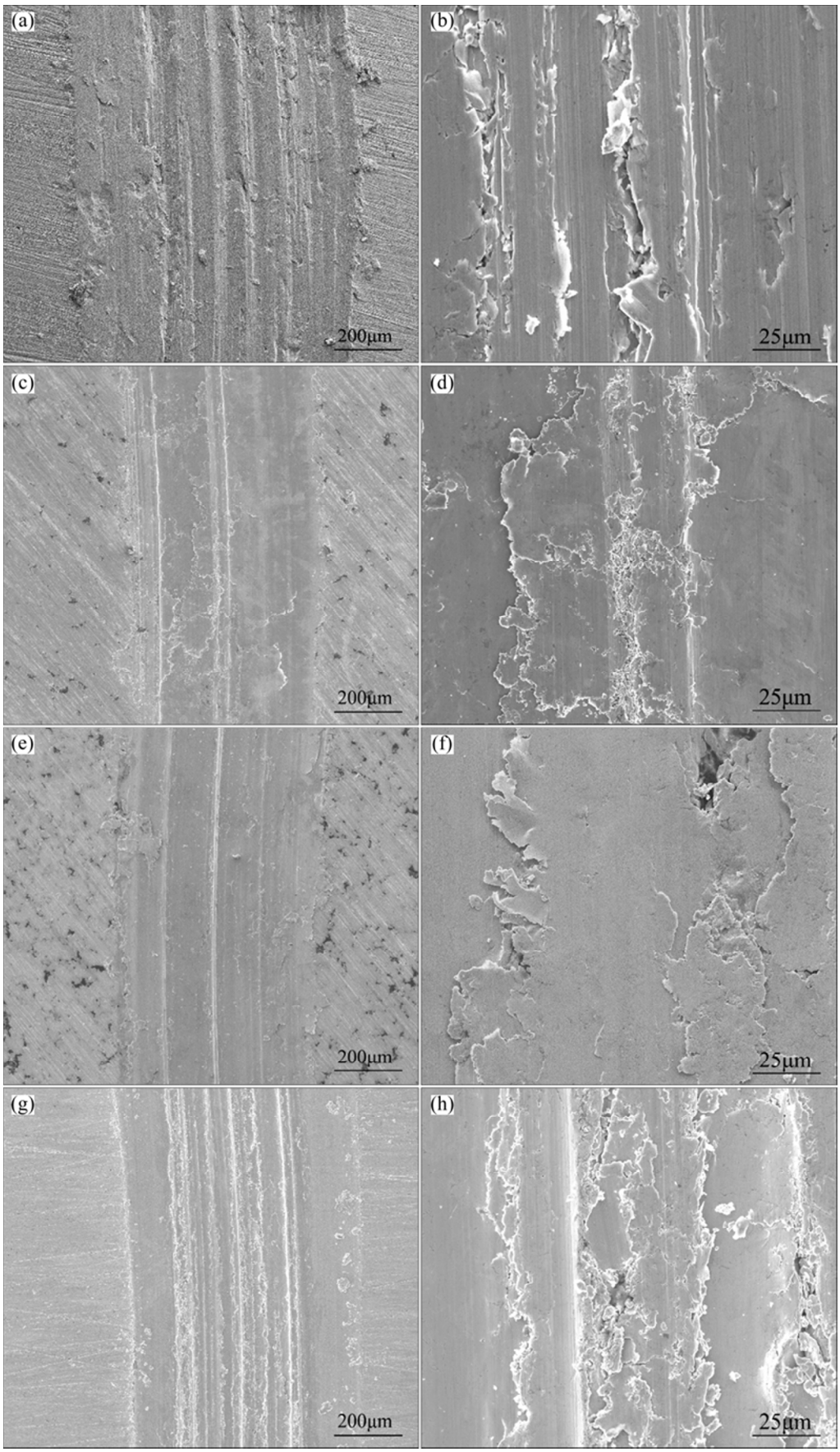

Fig. 6 Low (a, c, e, g) and high (b, d, f, h) magnification images of wear tracks of composites: (a, b) Cu−2.5%GNSs; (c, d) Cu−7.5%GNSs; (e, f) Cu−10%GNSs; (g, h) Cu−7.5%Gr

the low and high magnification images of the worn surfaces of Cu−2.5%GNSs, respectively. It is clear from Fig. 6(a) that the worn surface of the composite has a high order of roughness, besides, deep wear grooves along the sliding direction are observed, which suggests the wear mechanism is dominated by abrasion. The cracks and ploughing of materials which can be ascribed to the micro-cutting by hard wear debris entrapped in between the contact surfaces are detected, as shown in Fig. 6(b). These grooved lines and cracks on the worn surface illustrate the occurrence of plastic deformation. During sliding, considerable amount of plastic deformation occurs in the matrix, which results in the exposure of the GNSs particles to the contact surface. These GNSs particles are compacted with metal debris to form a thin tribolayer on the contact surface under normal load, which prevents further plastic deformation of the matrix and decreases the friction coefficient of the materials. However, for the composites containing lower volume fraction of GNSs, a strong adhesion between metals may occur during sliding due to insufficient supply of GNSs particles, resulting in high friction with severe surface damage.

The impact of reinforcement is advancing with increasing the GNSs content. During friction and wear test, the width of the wear track is directly proportional to the amount of material removed. In the case of Cu−7.5%GNSs composite, the appearance of worn surface is clearly smoother and the width of the wear track is comparatively lower, as shown in Fig. 6(c). This shows evidence of mild plastic deformation in the form of shallow grooves parallel to the sliding direction. It is well established that the wear rate can be minimized when the plastic deformation of material at the contact interface is prevented [26]. Delaminating scar and compacted tribolayer on the worn surface are observed in Fig. 6(d).

Figures 6(e) and (f) show the typical worn surfaces of Cu−10%GNSs composite. Compared with the specimen containing lower amount of GNSs (Cu−2.5%GNSs), the worn surface of Cu−10%GNSs composite has a higher flatness, although a few slim abrasive grooves can also be observed on the surface. In Fig. 6(f), the generation of cracks and cavities due to the delamination of surface materials is also found. The delamination involves subsurface deformation, crack nucleation and crack propagation [27]. The nucleation of cracks in the matrix is more likely to occur at weak points, namely, the interface between GNSs particles and copper matrix where pores can easily form, subsequently, crack propagation and interfacial debonding between the interface take place due to stress concentration during sliding, resulting in delamination wear. In general, the more the amount of Gu/GNSs interfaces, the more these processes arise. Therefore, the relatively higher proportion of Cu/GNSs interfaces may be responsible for the deterioration of mechanical properties and wear resistance of Cu−10%GNSs composite. However, with the wear rate increases, more GNSs may be exposed to the contact surface forming a compacted carbonaceous layer which has a self-lubricating ability and can partially avoid the direct metal to metal contact. As a result, the lowest as well as the most stable friction coefficient (Fig. 5(a)) is obtained by Cu−10%GNSs composite.

Figures 6(g) and (h) exhibit the typical worn surface of Cu−7.5%Gr composite. The worn surface is characterized by fairly surface damage and significant abrasive grooves, which indicates the Cu−Gr composite has load carrying capacity to a low extent. The grooves found on the surface may be attributed to the grinding of hard asperities of counter face or detached particles removed from the copper matrix.

Studying the shapes and sizes of wear debris provides clues to the wear mechanisms extant and brings information about the wear state. Figure 7(a) shows the SEM image of the wear debris of Cu−7.5%Gr composites. The delamination and abrasion wear-related flaky wear debris with 50−100 μm in dimension is observed, which indicates the occurrence of severe

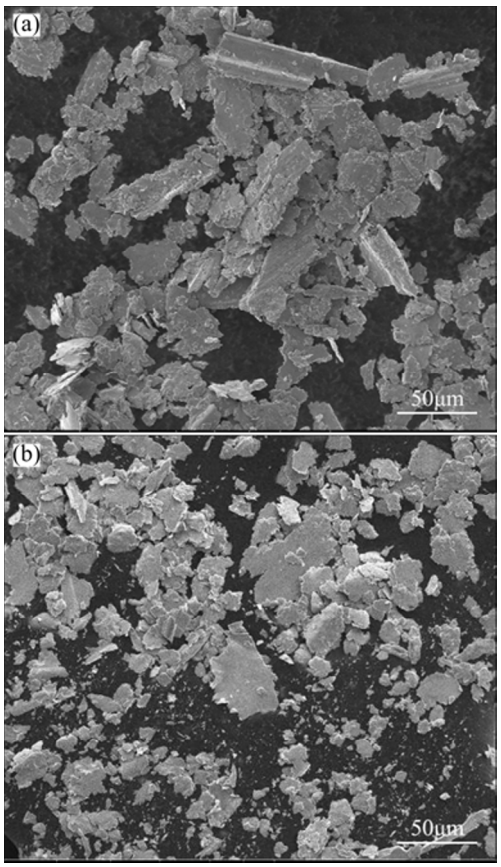

Fig. 7 SEM images of wear debris: (a) Cu−7.5%Gr; (b) Cu−7.5%GNSs

plastic deformation in Cu−7.5%Gr composite. According to fatigue wear theory [28], repeated sliding induces different stress fields between worn surface and subsurface, leading to the formation of highly plastically deformed area. Meanwhile, the cracks initiated from the weak points of the ultra-thin depth beneath the contact surface gradually grow and eventually shear to the surface, forming long thin wear fragments, as observed in Fig. 7(a).

Contrary to large wear debris, numerous fine particles as well as sheet-like wear debris with an average size of approximately 30 μm in planar are collected on the wear track of Cu−7.5%GNSs composite (Fig. 7(b)). The generation of fine wear debris is attributed to an abrasive micro-cutting effect. Generally, the appearance of smaller size of wear debris is related to better antiwear performance of the material [27] and this is consistent with the results of variation of wear rate shown in Fig. 4(b).

Raman spectroscopy reveals complementary information on the evolution of GNSs after each process, such as sintering and sliding. Thus Raman spectroscopy with an excitation laser energy of 2.41 eV (λ=514 nm) is performed on GNSs, as-prepared Cu−7.5%GNSs composite and the wear track of Cu−7.5%GNSs composite, respectively, as shown in Fig. 8. It is clear from Fig. 8 that the typical peaks of graphene are observed at ~1350 cm^{-1} (D band), ~1585 cm^{-1} (G band) and ~2700 cm^{-1} (2D band). In addition, there is a positive shift and broadening of G band of the worn surface of Cu−7.5%GNSs composite compared with the undamaged surface. This shift and broadening can be attributed to the residual strain in the GNSs [29,30], which is induced by the shear stress at the contact surface during sliding, resulting in the structure disruption of graphene. The copper matrix and the presence of debris on the wear track produce a wide fluorescence band that partially hides the distinct Raman features (2D peak) of the wear track of Cu−7.5%GNSs composite.

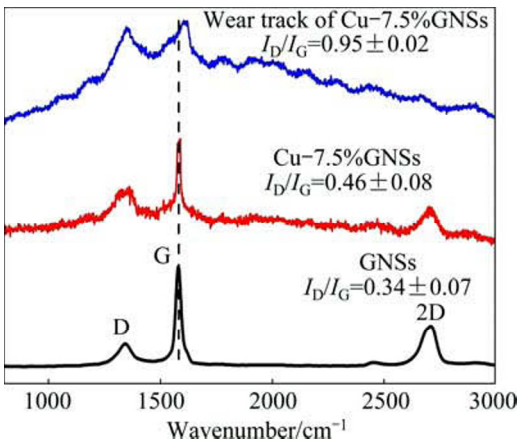

Fig. 8 Raman spectra of GNSs and Cu−7.5%GNSs composite without and with damaged surface (wear track)

When studying the disorder of graphene by Raman spectroscopy, the relative intensity (I) between the D and G bands is the main feature that is taken into consideration. As can be seen from Fig. 8, the I_D/I_G ratio increases marginally from 0.34 to 0.46 after sintering, which illustrates the successful retainment of GNSs with minimal structure damage, nevertheless, it reaches a maximum of 0.95 after sliding. The larger I_D/I_G ratio represents the higher defect density in graphitic structure, and therefore more exfoliated and fragmented GNSs flakes contribute to the formation of a lubricating tribolayer on the contact interface, resulting in improved wear resistance. Similar result has been observed by other authors for ceramic matrix composites containing graphene [16].

4 Conclusions

1) Cu−GNSs composites exhibit higher mechanical properties compared with Cu−Gr composites with the same volume fraction of GNSs and Gr. The inherent exotic properties such as superior strengthening effect of GNSs are responsible for the higher ranking of properties. Cu−10%GNSs composite shows poor mechanical properties due to the agglomeration effect. It is confirmed that the maximum volume fraction of GNSs to the copper matrix composites is limited to 7.5%.

2) GNSs reinforced copper matrix shows higher wear resistance and lower friction coefficient compared with Cu−Gr composites by forming a smoother and more compact lubricating tribolayer at the contact surface. A small amount of GNSs is sufficient to reduce the friction and wear of copper matrix composites drastically, which exhibits the remarkable lubricating efficiency, whereas graphite does not work well due to the limited content.

3) The Raman spectroscopy confirms the slight increase of I_D/I_G ratio of GNSs after sintering, indicating the GNSs are successfully retained with minimal structure damage during the hot pressing process. However, the I_D/I_G ratio reaches a maximum after sliding, which demonstrates the formation of a GNSs-rich lubricating tribolayer at the contact surface which hinders friction and wear.

References

[1] ZHAO H J, LIU L, WU Y T, HU W B. Investigation on wear and corrosion behavior of Cu−graphite composites prepared by electroforming [J]. Composites Science and Technology, 2007, 67: 1210−1217.

[2] ZAHRAN R R, IBRAHIM I H M, SEDAHMED G H. The corrosion of graphite/copper composites in different aqueous environments [J]. Material Letter, 1996, 28: 237−244.

[3] ROHATGI P K, RAY S, LIU Y. Tribological properties of metal matrix−graphite particle composites [J]. International Materials Reviews, 1992, 37(3): 129−149.
[4] RAJKUMAR K, ARAVINDAN S. Tribological behavior of microwave processed copper–nanographite composites [J]. Tribology International, 2013, 57: 282−296.
[5] KOVÁČIK J, EMMER Š, BIELEK J. Effect of composition on friction coefficient of Cu–graphite composites [J]. Wear, 2008, 265(3): 417−421.
[6] FUTAMI T, OHIRA M, MUTO H, SAKAI M. Contact/scratch-induced surface deformation and damage of copper–graphite particulate composites [J]. Carbon, 2009, 47(11): 2742−2751.
[7] AKHLAGHI F, ZARE-BIDAKI A. Influence of graphite content on the dry sliding and oil impregnated sliding wear behavior of Al 2024–graphite composites produced by in situ powder metallurgy method [J]. Wear, 2009, 266(1): 37−45.
[8] DONNET C, ERDEMIR A. Solid lubricant coatings: Recent developments and future trends [J]. Tribology Letters, 2004, 17(3): 389−397.
[9] RAJKUMAR K, ARAVINDAN S. Tribological studies on microwave sintered copper–carbon nanotube composites [J]. Wear, 2011, 270(9): 613−621.
[10] RAPOPORT L, LESHCHINSKY V, LVOVSKY M. Friction and wear of powdered composites impregnated with WS_2 inorganic fullerene-like nanoparticles [J]. Wear, 2002, 252(5): 518−527.
[11] LEE C, LI Q, KALB W, LIU X Z, BERGER H, CARPICK R W, HONE J. Frictional characteristics of atomically thin sheets [J]. Science, 2010, 328(5974): 76−80.
[12] GEIM A K, NOVOSELOV K S. The rise of graphene [J]. Nature Materials, 2007, 6(3): 183−191.
[13] SINGH E, THOMAS A V, MUKHERJEE R, MI X, HOUSHMAND F, PELES Y, KORATKAR N. Graphene drape minimizes the pinning and hysteresis of water drops on nanotextured rough surfaces [J]. ACS Nano, 2013, 7(4): 3512−3521.
[14] XU Z, SHI X, ZHAI W, YAO J, SONG S, ZHANG Q. Preparation and tribological properties of TiAl matrix composites reinforced by multilayer graphene [J]. Carbon, 2014, 67: 168−177.
[15] SHIN Y J, STROMBERG R, NAY R, HUANG H, WEE A T, YANG H, BHATIA C S. Frictional characteristics of exfoliated and epitaxial graphene [J]. Carbon, 2011, 49(12): 4070−4073.
[16] PORWAL H, TATARKO P, SAGGAR R, GRASSO S, MANI M K, DLOUHÝ I, REECE M J. Tribological properties of silica–graphene nano-platelet composites [J]. Ceramics International, 2014, 40(8): 12067−12074.
[17] BERMAN D, ERDEMIR A, SUMANT A V. Reduced wear and friction enabled by graphene layers on sliding steel surfaces in dry nitrogen [J]. Carbon, 2013, 59: 167−175.
[18] BERMAN D, ERDEMIR A, SUMANT A V. Few layer graphene to reduce wear and friction on sliding steel surfaces [J]. Carbon, 2013, 54: 454−459.
[19] PORWAL H, GRASSO S, REECE M J. Review of graphene−ceramic matrix composites [J]. Advances in Applied Ceramics, 2013, 112(8): 443−454.
[20] PORWAL H, GRASSO S, CORDERO-ARIAS L, LI C, BOCCACCINI A R, REECE M J. Processing and bioactivity of 45S5 Bioglass®−graphene nanoplatelets composites [J]. Journal of Materials Science: Materials in Medicine, 2014, 25(6): 1403−1413.
[21] KHAN U, MAY P, PORWAL H, NAWAZ K, COLEMAN J N. Improved adhesive strength and toughness of polyvinyl acetate glue on addition of small quantities of graphene [J]. ACS Applied Materials and Interfaces, 2013, 5(4): 1423−1428.
[22] LIN J, WANG L, CHEN G. Modification of graphene platelets and their tribological properties as a lubricant additive [J]. Tribology Letters, 2011, 41(1): 209−215.
[23] ZHAI W, SHI X, WANG M, XU Z, YAO J, SONG S, WANG Y. Grain refinement: A mechanism for graphene nanoplatelets to reduce friction and wear of Ni_3Al matrix self-lubricating composites [J]. Wear, 2014, 310(1): 33−40.
[24] SHAFIEI M, ALPAS A T. Effect of sliding speed on friction and wear behavior of nanocrystalline nickel tested in an argon atmosphere [J]. Wear, 2008, 265(3): 429−438.
[25] KIM W J, LEE T J, HAN S H. Multi-layer graphene/copper composites: Preparation using high-ratio differential speed rolling, microstructure and mechanical properties [J]. Carbon, 2014, 69: 55−65.
[26] KUMAR K A, PILLAI U T, PAI B C, CHAKRABORTY M. Dry sliding wear behavior of Mg−Si alloys [J]. Wear, 2013, 303(1): 56−64.
[27] ZHANG J, ALPAS A T. Delamination wear in ductile materials containing second phase particles [J]. Materials Science and Engineering A, 1993, 160(1): 25−35.
[28] BRAUNOVIC M, MYSHKIN N K, KONCHITS V V. Electrical contacts: Fundamentals, applications and technology [M]. Florida: CRC Press, 2006: 57−58.
[29] TSOUKLERI G, PARTHENIOS J, PAPAGELIS K, JALIL R, FERRARI A C, GEIM A K, GALIOTIS C. Subjecting a graphene monolayer to tension and compression [J]. Small, 2009, 5(21): 2397−2402.
[30] LIAO J, TAN M J. Mixing of carbon nanotubes (CNTs) and aluminum powder for powder metallurgy use [J]. Powder Technology, 2011, 208(1): 42−48.

石墨烯和石墨增强铜基复合材料的摩擦磨损性能

李景夫，张 雷，肖金坤，周科朝

中南大学 粉末冶金国家重点实验室，长沙 410083

摘 要：采用热压方法制备不同石墨烯含量的铜−石墨烯复合材料，并将其力学性能和摩擦磨损性能与用相同方法制备的铜−石墨复合材料进行对比。实验结果表明：当复合材料中石墨与石墨烯体积分数相同时，铜−石墨烯复合材料具有更高的相对密度、显微硬度以及抗弯强度。随着铜−石墨烯复合材料中石墨烯含量的增加，材料的摩擦系数及磨损率明显降低，而铜−石墨复合材料中石墨的减磨作用较小。两种复合材料的磨损机制主要为磨粒磨损和疲劳磨损。铜−石墨烯复合材料优异的力学性能和摩擦磨损性能得益于石墨烯高的润滑效率及其对铜基体的增强作用，这表明石墨烯是铜基复合材料的理想添加剂，不仅可以作为有效的润滑剂，还可以作为良好的强化相。

关键词：石墨烯纳米片；石墨；复合材料；摩擦系数；磨损机制

(Edited by Mu-lan qin)